

REDSHIFT AND THE SHAPE OF THE UNIVERSENathan Burwig¹, Maxwell Kaye² and Krzysztof Sliwa

Tufts University

Department of Physics and Astronomy
Medford, Massachusetts 02155 USA**Abstract**

Hubble's observation in 1929 that redshifts of far-away objects increase with their distance is customarily interpreted as being due to expansion of the universe, leading to the universally accepted ideas of the Big Bang and a spatially flat, infinite universe. We explore an alternative model of the universe, proposed by Segal in 1972, which has geometry $\mathbb{R} \times S^3$. It is eternal, not expanding, and is spatially curved, compact and finite, as in the Einstein static universe. Our preliminary analysis of open source datasets shows that the model's predictions are consistent with two important types of cosmological data: cosmological redshift and cosmic background radiation. With new data from the James Webb Space Telescope, verification of predictions that distinguish the standard model from Segal's model of the universe is increasingly feasible.

¹now at Arizona State University, Tempe, Arizona, USA²now at McGill University, Department of Mathematics and Statistics, Montreal, Canada

INTRODUCTION

16 In 1929, Hubble [1] showed that the redshift in the light spectra of far-away nebulae, first observed by Slipher,
17 is proportional to their distances from Earth. Hubble suggested that in the de Sitter cosmology this effect could be
18 analogous to the familiar Doppler effect, except this cosmological redshift is not caused by objects receding from each
19 other in space, but by the stretching of space itself. In 1935, Hubble and Tolman [2] considered the expansion of the
20 universe as one of possible explanations for the redshift-distance relation observed by Hubble. They also mentioned
21 a possibility that the increase of redshift with distance could be caused by some other unknown effect due to the
22 geometry of the universe. However, no definitive explanation of this kind was found at the time, and the expanding
23 universe hypothesis became accepted as a fact.

24 In the Lambda Cold Dark Matter Model (Λ CDM), also known as the Standard Cosmological Model (SCM),
25 acceptance of this hypothesis led to the ideas of the Big Bang and inflation. The shape of the universe is assumed
26 to be spatially flat, $M_0 = \mathbb{R} \times \mathbb{R}^3$. In 1972, Irving Segal proposed an alternative explanation for the observed
27 increase of redshifts with the distance of far-away objects [3]. The axioms of physical symmetries—global isotropy
28 and homogeneity of space and time, and its causality properties, are satisfied not only by Minkowski spacetime,
29 $\mathbb{R} \times \mathbb{R}^3$, but also by a universe whose geometry is $\mathbb{R} \times S^3$. It is the geometry of the Einstein static universe -
30 non-expanding, spatially closed, finite, and eternal. Einstein abandoned this model after the increase of redshift with
31 distance became accepted as evidence for expansion of the universe. The two geometries are indistinguishable locally,
32 even across intergalactic distances, with observable differences appearing only on cosmological scales.

33 The two universes and their causal structure are deeply connected, and their relationship gives rise to possible
34 observable differences. Not only is $\mathbb{R} \times \mathbb{R}^3$ the tangent space to each observer in $\mathbb{R} \times S^3$, but Minkowski space
35 can be causally embedded in Segal's universe. This means that an observer of events in $\mathbb{R} \times S^3$ would observe a
36 time-orientation preserving set of events by observing their stereographic projection onto their local Minkowski space,
37 tangent to $\mathbb{R} \times S^3$ at observer's location. Segal postulates that observations are indeed made in this local Minkowski
38 projection, and from this hypothesis, shows that redshift arises naturally. This theory provides a verifiable prediction
39 for the dependence of this geometric redshift on the geodesic distance light travels through in $\mathbb{R} \times S^3$, which is distinct
40 from the redshift-distance relation provided by the Λ CDM theory.

41 A concise introductory overview of Segal's theory was given by Daigneault and Sangalli [4]. A detailed review of
42 Segal's book was written by Taub [5]. References to Segal's papers and books on Chronometric Cosmology can be
43 found in the bibliography[3,6-34].

44 Segal's work was not accepted by his contemporaries. They raised both theoretical and empirical concerns about
45 chronometric cosmology [16, 25], which Segal addressed [17, 26], but the conversation died out. In the modern day,
46 with newly available data that is more precise and farther reaching, we seek to reopen the question of chronometric
47 cosmology and consider if it can be falsified in the modern context. Surprisingly, the currently available data does
48 not falsify Segal's model.

SEGAL'S CHRONOMETRIC COSMOLOGY

49 Segal's original motivation was to explore possible generalizations of Minkowski space-time of special relativity to
50 some other 4-dimensional manifold, given that Maxwell's equations are not only Lorentz invariant but also conformally
51 invariant. The Poincaré group and Minkowski space-time would then be a limiting case of a more accurate theory,
52 similarly to the Galilean group being a limit of the Lorentz group when the speed of light approaches infinity.

53 Lie algebras of pseudo-orthogonal groups $O(1, 5)$, $O(2, 4)$, and $O(3, 3)$ are deformable into that of the fundamental
54 dynamical variables (momenta, boosts, and space-time coordinates) in relativistic quantum mechanics [6]. As pointed
55 out by Segal [7], $O(1, 5)$ which is the group of de Sitter space, is difficult to reconcile with the principle of positivity
56 of the energy in quantum mechanics as it does not have a self-adjoint generator correspond to a nonnegative energy
57 in any nontrivial unitary representation of $O(1, 5)$. The group $O(2, 4)$, the conformal group of Minkowski space is a
58 candidate for a more accurate higher symmetry group as it is free from this deficiency. In 1971, Segal observed that
59 the acausality of conformal spacetime could be remedied through its replacement by the locally identical section of
60 the universal covering space [8].

61 Segal's cosmology [13] is based on the following assumptions:

- 62 ● space-time is 4-dimensional manifold
- 63 ● space-time has causal structure: (a) at each point of the universe there is given a convex cone of infinitesimal
64 future directions in the tangent space to the manifold at that point; (b) there are no closed timelike loops.
- 65 ● space-time is causally spatially isotropic: at any point of spacetime there is no preferred spacelike direction
66 (this assumption does not imply spatial uniformity in the distribution of matter)
- 67 ● space-time is causally temporally isotropic: there is no preferred timelike direction at any point of spacetime.
68 For any two timelike directions at a given point of spacetime, there is a causal diffeomorphism of spacetime
69 onto itself that maps one of these directions on the other

- 70 • spacetime can be globally factorized into *time* \times *space*
- 71 • spacetime is causally temporarily homogenous: translations with respect to the *time* \times *space* factorization
- 72 form up a group of causal automorphisms of spacetime, the temporal group belonging to this factorization;
- 73 the energy is invariant under a group of *causal* temporal translations related to a factorization of spacetime as
- 74 *time* \times *space*
- 75 • spacetime is spatially homogenous

76 Segal showed [13] that these axioms are satisfied by only two possible manifolds: Minkowski $M_0 = \mathbb{R} \times \mathbb{R}^3$ and

77 $M = \mathbb{R} \times S^3$.

78 The group $SO(2, 4)$ is the 15-parameter conformal group of Minkowski space-time. (Sometimes its double cover

79 $SU(2, 2)$ is chosen, which is locally isomorphic to $SO(2, 4)$.) The Lie Algebra $so(2, 4)$ is composed of 10 Poincare

80 generators, $M_{\mu\nu}$ (space rotations and boosts) and P_μ (translations), together with scale transformation D and special

81 conformal generators K_μ . By a theorem by Alexandrov and Zeeman [37], causality preserving transformations on

82 Minkowski space are conformal transformations.

83 One can compactify the Minkowski space M_0 , with $O(1, 3)$ as its symmetry group, by including it into the

84 projective light cone (i.e. the space of all null lines through the origin) in a 6-dimensional Euclidean space $\mathbb{R}^2 \times \mathbb{R}^4$

85 with (2,4) signature [13]. The group $SO(2, 4)$ naturally acts on this space. Segal discussed compactification of

86 Minkowski space in two ways: as a manifold with a $U(2)$ group action; and as a projective quadric in 6-dimensional

87 real space of signature (2, 4).

88 Darboux [35] introduced higher-dimensional *polyspherical* coordinates for higher-dimensional spaces with a point

89 at ∞ included. Given $x^0, x^1, x^2, \dots, x^{n-1}, k, q \in \mathbb{R}$, with $x^0, x^1, x^2, \dots, x^{n-1}$ the Cartesian coordinates of a space \mathbb{R}^n

90 with a Euclidean or pseudo-Euclidean metric form, one can define *polyspherical* coordinates y^0, y^1, \dots, y^{n+1} by

$$91 \begin{cases} y^\mu = x^\mu k, & \mu = 0, \dots, n-1 \\ y^n = (k+q)/2, & y^{(n+1)} = (k-q)/2 \end{cases} \quad (1)$$

92 If the metric is Lorentzian,

$$93 (x, x) = (x^0)^2 - (x^1)^2 - (x^2)^2 - \dots - (x^{n-1})^2, \quad (2)$$

94 then the associated bilinear quadratic form in *polyspherical* coordinates is

$$95 Q(y, y) = (y^0)^2 + (y^{n+1})^2 - (y^1)^2 - (y^2)^2 - \dots - (y^n)^2, \quad k = y^n + y^{n+1}, \quad q = y^n - y^{n+1}. \quad (3)$$

106 The light-cone at any point of Minkowski space is defined by a set of null-vectors $g(x, x) = 0$, with g a metric form.
 107 Similarly, a quadric Q in \mathbb{R}^6 with the $SO(2, 4)$ action defines a natural Lorentz structure, which remain invariant
 108 under the action of $SO(2, 4)$ group. The group of causal conformal transformations on \mathbb{R}^6 are those for which
 109 $Q(y, y) = 0$. One can rewrite

$$100 \quad Q(y, y) = -(y^0)^2 - (y^5)^2 + (y^1)^2 + (y^2)^2 + (y^3)^2 + (y^4)^2, \quad (4)$$

101 which shows that the conformal group is related to the group $O(2, 4)$. Because the coordinate sets $(y^0, y^1, y^2, y^3, k, q) \simeq$
 102 $\lambda(y^0, y^1, y^2, y^3, k, q)$ are equivalent up to a multiplicative factor λ with points in Minkowski space M_0 , one can rewrite
 103 $Q(y, y) = 0$ as

$$104 \quad (y^0)^2 + (y^5)^2 = 1 = (y^1)^2 + (y^2)^2 + (y^3)^2 + (y^4)^2. \quad (5)$$

105 Thus the compactified Minkowski space on which the conformal group acts continuously is compact and topologically
 106 isomorphic to $\overline{M} \simeq (S^1 \times S^3)/\mathbb{Z}_2$, or that time is compactified to S^1 and space to S^3 . Time becomes periodic. To
 107 avoid this, one has to use the universal covering space $M \simeq \mathbb{R} \times S^3$ and find the correspondence between six
 108 *polyspherical* coordinates on \mathbb{R}^6 and four coordinates in Minkowski space M_0 .

109 The manifold $\widetilde{M} = S^1 \times S^3$ is the two-fold covering space of \overline{M} , while $M = \mathbb{R} \times S^3$ covers it infinite number
 110 of times. The Minkowski space M_0 can thus be regarded as an open dense submanifold of \overline{M} which is covered
 111 infinitely many times by M . The space $S^1 \times S^3$ admits a local notion of causality, but it not causal globally. The
 112 space $\mathbb{R} \times S^3$ is the universal covering space of the conformal compactification \overline{M} of Minkowski space M_0 which is
 113 globally causal [13].

Minkowski space M_0 can also be compactified as the group manifold of the unitary group $U(2)$ via the Cayley transform. Minkowski spacetime can be represented by the causally isomorphic real linear space $H(2)$ of 2×2 Hermitian matrices. For a point $P \in M_0$ with coordinates $(x^0 := ct, x^1, x^2, x^3)$, with c the speed of light, the corresponding matrix A is:

$$A = \begin{pmatrix} x^0 + x^3 & x^1 + ix^2 \\ x^1 - ix^2 & x^0 - x^3 \end{pmatrix} \in H(2)$$

114 This defined a map $\alpha : M_0 \rightarrow H(2)$. The vector space $H(2)$ of 2×2 Hermitian matrices can be causally immersed
 115 as a dense subset of the compact group $U(2)$ of 2×2 unitary matrices as follows. For a Hermitian matrix A , the
 116 Cayley transform $U(A)$ is the corresponding matrix:

$$117 \quad U(A) = (\mathbb{I} + \frac{1}{2}iA)(\mathbb{I} - \frac{1}{2}iA)^{-1} \quad (6)$$

118 where \mathbb{I} is the identity matrix. The Cayley transform, $\beta : A \mapsto U(2)$, is one-to-one and, importantly, causal. It has a

119 unique inverse, which is the generalized stereographic projection,

$$120 \quad A = -2i(U - \mathbb{I})(U + \mathbb{I})^{-1}, \quad (7)$$

121 well defined as long as $\det(U + \mathbb{I}) \neq 0$. The generalized stereographic projection is an analogue of the mapping
 122 between the unit circle in the complex plane, a multiplicative Lie group, and the imaginary axis its Lie algebra. The
 123 conformal infinity is the subset of $U(2)$ consists of those matrices $U \in U(2)$ for which $\det(U + \mathbb{I}) = 0$. The group
 124 $SU(2, 2)$ acts naturally on $U(2)$.

125 The compactification $U(2)$ of $H(2)$ can be lifted to its universal covering space $M = \mathbb{R} \times S^3$. The group $SU(2)$
 126 is isomorphic to unit quaternions and is thus diffeomorphic to S^3 , and $U(2) \simeq U(1) \times SU(2)$. More precisely, the
 127 quotient $U(2)/SU(2)$ is isomorphic to $U(1)$. The group $SU(2)$ is diffeomorphic to S^3 , thus $U(2) \simeq S^1 \times S^3$. Since
 128 Minkowski spacetime is isomorphic to $H(2)$, it follows that $\mathbb{R} \times S^3$ is the covering space of the compactification of
 129 Minkowski spacetime, $\mathbb{R} \times \mathbb{R}^3$. The following sequence of mappings [36] causally immerses Minkowski spacetime M_0
 130 into the Segal-Einstein universe M :

$$131 \quad M_0 = \mathbb{R} \times \mathbb{R}^3 \xrightarrow{\alpha} H(2) \xrightarrow{\beta} U(2) \xrightarrow{\gamma} \mathbb{R} \times SU(2) = \mathbb{R} \times S^3 = M. \quad (8)$$

SEGAL'S COSMOLOGICAL REDSHIFT

132 Minkowski space M_0 can be thought of as the tangent space at any point of $\mathbb{R} \times S^3$, just as the complex plane
 133 is tangent to the Riemann sphere. However, the immersion of M_0 into $\mathbb{R} \times S^3$ does not preserve the time coordinate
 134 or the space coordinates in the factorizations of these space-times as "space \times time".

135 Local observations of dynamical quantities are represented not necessarily by generators of true, global symmetries,
 136 but by generators of corresponding symmetries in the flat tangential space. While angular momenta remain unchanged,
 137 the energy and linear momenta differ. The true energy is no longer represented by $-i\hbar \frac{\partial}{\partial t}$, but by an operator $-i\hbar \frac{\partial}{\partial \tau}$
 138 where τ is the global time. Time and energy differ crucially in the two models [13] .

139 Assuming that the global, physical time τ is that derived from the $\mathbb{R} \times S^3$ factorization, and that Minkowski
 140 time t is only a local projection of it, the redshift of photons propagated over large distances is obtained from the
 141 conformal invariance of Maxwell's equations and the requirement that the action of the time evolution groups, both
 142 standard (Minkowski) and non-standard ($\mathbb{R} \times S^3$), is unitary. The global time τ and Minkowski's time t coordinates
 143 are related by the equation [13]

$$144 \quad t = \frac{2R}{c} \tan\left(\frac{c\tau}{2R}\right) \quad (9)$$

145 where R is the radius of a 4-dimensional ball whose boundary S^3 constitutes our 3-dimensional space, and c is the
 146 speed of light. The two times correspond to two concepts of energy. The global, cosmic energy in $\mathbb{R} \times S^3$ is conserved,
 147 while the photon energy measured in Minkowski $\mathbb{R} \times \mathbb{R}^3$ is reduced by the redshift. The redshift-distance relation in
 148 Segal's model [13] constitutes a verifiable prediction of the dependence of this redshift z on the geodesic distance
 149 $l = c\tau$ on S^3

$$150 \quad z = \tan^2 \left(\frac{c\tau}{2R} \right) = \tan^2 \left(\frac{\rho}{2} \right) \quad (10)$$

151 The dimensionless quantity $\rho = l/R$, or a 4-dimensional analogue of the polar angle, runs from 0 to π when light
 152 is traveling from the emission point to its antipode in S^3 . The redshift becomes infinite when the light goes around
 153 through a half-turn around the $\mathbb{R} \times S^3$ universe to the observer. The redshift-distance relation can be also derived
 154 geometrically [28].

SEGAL'S COSMOLOGY, MATTER AND INTERACTIONS

155 In the $\mathbb{R} \times S^3$ space-time, Maxwell's equations remain intact, as they are conformally invariant. The solutions
 156 to Maxwell's equations in Minkowski space extend uniquely to their solutions in the $\mathbb{R} \times S^3$ universe [23]. The same
 157 holds for the Dirac equation, and for the Yang-Mills equations, which describe fermions and the strong and weak
 158 interactions in particle physics. These equation are conformally invariant in absence of matter, which allows to relate
 159 the Dirac and Young-Mills theories on Minkowski space-time with their analogues on a manifold with the boundary.

160 Special relativity is a limiting case of Segal's conformal theory, as the radius R becomes infinity. Locally, the two
 161 geometries are indistinguishable. Einstein's general relativity relates gravitation to curvature of space. In Einstein's
 162 original equations, flat Minkowski space is the simplest solution to the vacuum field equations of an empty universe.
 163 Einstein's modified equations include a cosmological constant term introduced to allow for a non-expanding universe
 164 in the presence of matter. However, the modified equations are the most general equations satisfying the usual
 165 minimal conditions. They allows for an empty space to have curvature, as in Segal's model. The inclusion of this
 166 term does not result in any inconsistencies with General Relativity. The relation of Segal's universe to general relativity
 167 is analogous to that for special relativity, except that the geometry of empty space is $\mathbb{R} \times S^3$ rather than $\mathbb{R} \times \mathbb{R}^3$. In
 168 the limit of $R \rightarrow \infty$, the $M = \mathbb{R} \times S^3$ universe becomes Minkowski $M_0 = \mathbb{R} \times \mathbb{R}^3$ spacetime. Segal's theory does
 169 not assume general relativity, but is compatible with it [13].

170 To quote Segal himself [19]: "How is general relativity and its relation to cosmology affected? The postulated
 171 infinitesimal structure of space-time in general relativity, i.e. of reference or empty space-time, is changed from a
 172 Minkowski space, formed from the tangent space at the point of observation, to a chronometric space, $\mathbb{R} \times S^3$,

173 invariantly attached to the point as the universal covering space of the conformal compactification of the tangent
174 space with respect to the metric given in it. As far as is now known, the radius of the S^3 is too large (in conventional
175 units; in natural units, the S^3 is of unit radius) to produce any presently observable effects in the small, and local
176 observable aspects of general relativity are therefore unaffected. In the large, because of the compactness of S^3 it is
177 necessary, as Einstein proposed, to add the cosmological term to his equation. Overall, the resulting universe departs
178 widely from the Friedman-Lemâitre model—any expansion, if present at all, must be slight-but in its gross features
179 is consistent with Einstein’s original static conception.”

PRELIMINARY COMPARISONS OF MODELS OF UNIVERSE WITH DATA

180 The predicted redshift-distance relations are different in Segal’s model and in the expansionary SCM model [38,39].
181 At least in principle, the data itself can differentiate between the two models. Segal published several papers showing
182 that the data available at his time agreed with the predictions of his $\mathbb{R} \times S^3$ universe. However, since his passing
183 in 1998, enormous progress has been made in observational astronomy. Modern galactic surveys are covering larger
184 areas of the sky and and provide data from greater redshifts than have been probed previously. Here, we set out to
185 investigate whether Segal’s model can be falsified with modern data.

THE MAGNITUDE-REDSHIFT RELATION

186 For distant objects, distance is not a directly observable quantity, and it can only be estimated using various
187 proxies. If one assumes that the objects are standard candles with the same absolute luminosity, the purely geometric
188 relations between apparent luminosity and distance allows comparison of correlations between the observed magnitude
189 and redshift, $m(z)$. The data for type 1a supernovae, the best known standard candles, agrees very well with the SCM,
190 but it also agrees with Segal’s model. In Figure 1, the data from the Supernova Cosmology Project [40] compilation
191 Union2.1 is shown along with theoretical predictions from the SCM (red) and from Segal’s $\mathbb{R} \times S^3$ cosmology (green).
192 More information about the theoretical predictions used, and the fits themselves can be found in Appendix 1.

193 One should keep in mind that the comparison, although in principle very simple, is not trivial due to possible but
194 unknown effects of extinction of light from distant sources and details of star evolution in time.

THE NUMBER COUNT $N(< z)$ RELATION

195 Another independent observable is the number count, or the number of objects of a given type seen in a fixed
196 cone versus their redshift, $N(< z)$. Assuming a uniform distribution of objects in the universe, $N(< z)$ is directly

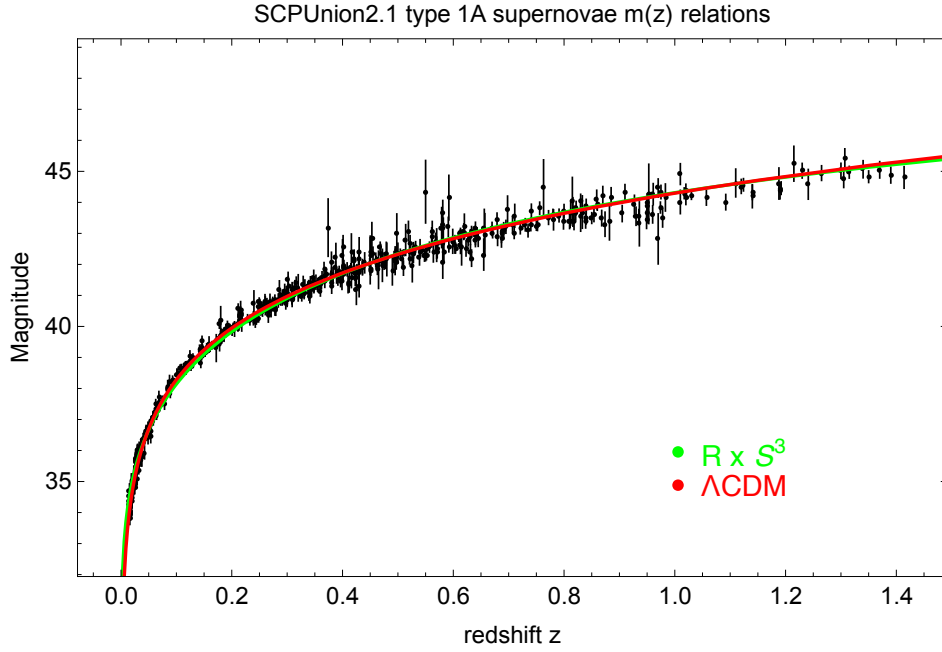


Figure 1: The SCP "Union2.1" SN Ia compilation is an update of the "Union2" compilation. Plotted are observed magnitudes as a function of redshift for 580 SNe type Ia that pass usability cuts. The red curve is the result of fits based on Standard Cosmological Model [38] of $m(z)$ within SCM with $q_0 = 1/2$ for a flat space, and including a correction for possible light extinction. The green curve is based on Segal's model $\mathbb{R} \times S^3$. The prediction from Segal's model includes a correction for the observed intensity to account for possible extinction, $I_{corr} = I \exp(-\lambda c\tau)$, corresponding to the extinction length of $1/\lambda \approx \frac{1}{2}R$, the radius of the universe. The two fits have the same number of free parameters. Fits to a newer parametrization [39], assuming zero curvature term $\Omega_k = 0$, and taking $\Omega_{matter} = 0.276$ for the matter term (red), as determined independently from the CMB studies, gives virtually identical results to those obtained with the SCM parametrization used in the fit [38].

197 proportional to the volume, $V(< z)$, enclosed in this cone, and is thus sensitive to the geometry of space. Plotting
198 $N(< z)/N(< z_{max})$, where z_{max} is the maximum redshift in a sample, and comparing it to $V(< z)/V(< z_{max})$ as
199 a function of redshift z can, in principle, differentiate between possible geometries of the universe.

200 The data from several Astrodeep Hubble Frontier Fields [41], based on a combination of observations from the
201 Hubble Space Telescope, the Spitzer telescope, and the ground-based VLT Hawk-I is found to be in agreement
202 with predictions of Segal's model. In Figure 2, we show results on $N(< z)$ as a function of the redshift z for the
203 Astrodeep Abell 2744 field, and in Figure 3 we show the magnitude-redshift relation, $m(z)$, based on the same data,
204 for completeness. We selected only those objects in the Astrodeep Abell 2744 field that have redshifts determined
205 spectroscopically, or photometrically with the redshift uncertainty range $ZBEST_SIQR < 0.1$.

206 One should keep in mind that such comparisons may be affected by selection biases, by the unknown effects of
207 extinction of light when it travels through distant parts of the universe, and by possible effects due to evolution of
208 galaxies in time. For very large redshifts, there should be no galaxies in the SCM, as they need some minimum time
209 to form after the Big Bang.

210 Interestingly, several recent papers based on data obtained with the James Webb Space Telescope, reported
211 observations of distant galaxies of uncharacteristically large mass, given their high redshifts [42, 43]. According to
212 the current ideas about evolution of galaxies in the expanding universe, such objects are not expected so early after
213 the Big Bang. However, the presence of galaxies this large at such high redshifts is consistent with a static $\mathbb{R} \times S^3$
214 universe, in which galaxies are distributed homogeneously in the S^3 space, including distances corresponding to very
215 large redshift values.

THE COSMIC MICROWAVE RADIATION

216 It is an important observational fact that our universe is filled with omnidirectional cosmic microwave background
217 radiation (CMB) with the black body spectrum corresponding to temperature of approximately $T = 2.7 K$. In the
218 Λ CDM model, the CMB is explained as the light that was originally emitted from the surface of last scattering
219 about 380,000 years after the Big Bang, now at redshift of $z \sim 1100$ [44].

220 In Segal's model the CMB corresponds to "residual light", light that has not been absorbed over multiple turns
221 around the spatially closed $\mathbb{R} \times S^3$ universe. Segal has shown that its energy distribution is expected to be the Planck
222 black-body spectrum [23]. The only properties of light required in the proof are that it is described by Maxwell's
223 equations, Bose-Einstein statistics, and that it is stochastically emitted and absorbed by matter via a temporally
224 invariant interaction over many turns around the $M = \mathbb{R} \times S^3$ universe.

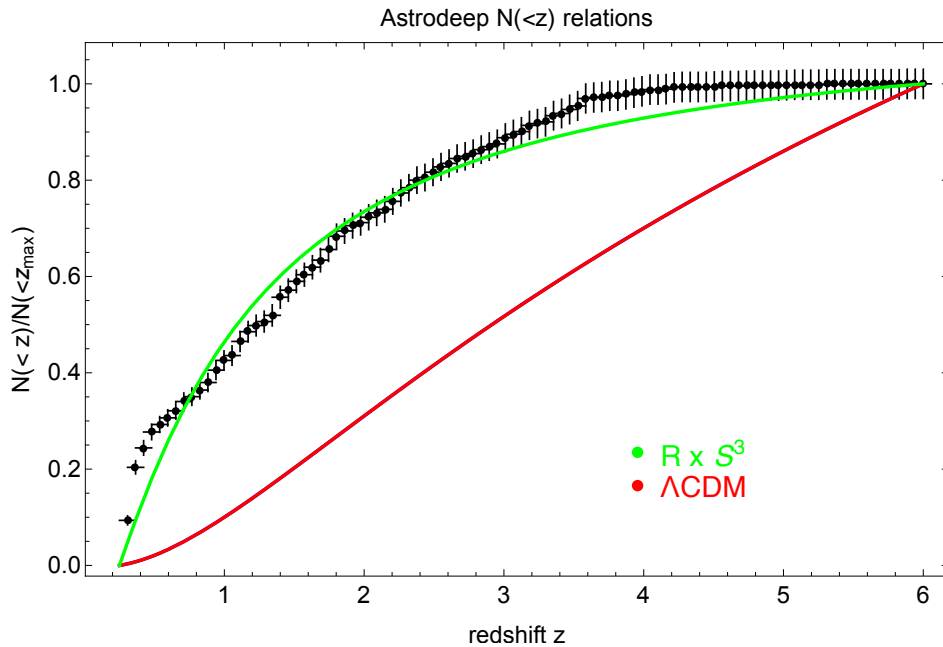


Figure 2: The normalized number count, $N(<z)/N(<z_{max})$ based on data from for one of Frontier Fields, Abell A2744, for objects that have their redshifts measured spectroscopically, or photometrically with the redshift uncertainty range $ZBEST_SIQR < 0.1$. The curves are the normalized volumes as a function of redshift z , $V(<z)/V(<z_{max})$ calculated for SCM (red) and Segal's $\mathbb{R} \times S^3$ cosmology (green). The number count $N(<z)$ is proportional to the volume, $V(<z)$, enclosed in a chosen angular cone up to redshift z . The dependence of the volume contained within redshift z is $V(<z) \sim (1 - \frac{1}{\sqrt{1+z}})^3$ for SCM [38], and $V(<z) \sim \tan^{-1}\sqrt{z} - \frac{1}{4}\sin(4\tan^{-1}\sqrt{z})$ for Segal's model [13], correspondingly.

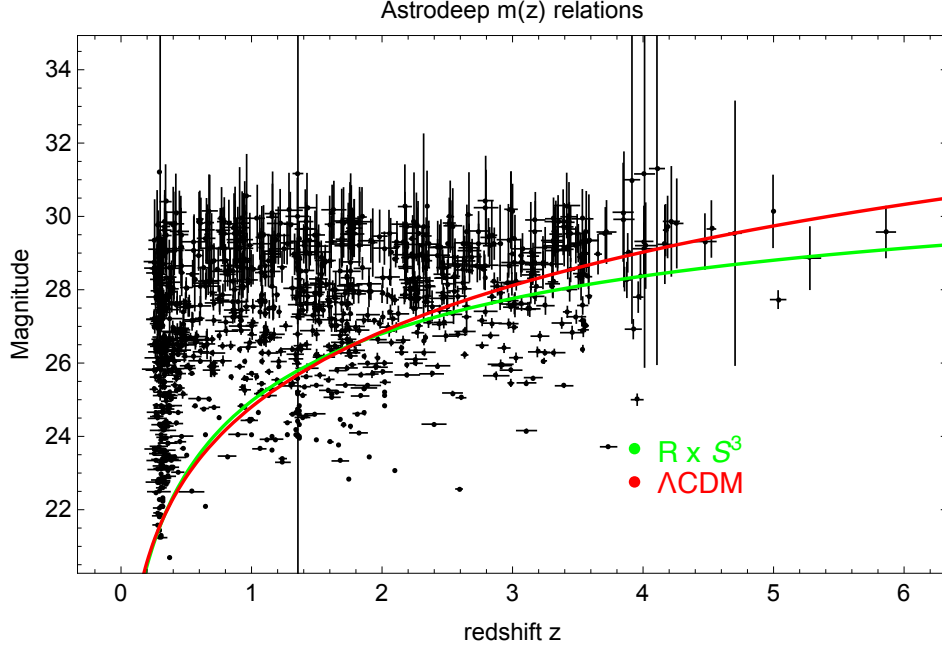


Figure 3: The observed magnitude as a function of redshift for objects from one of Frontier Fields, Abell A2744, for objects that have their redshifts measured spectroscopically, or photometrically with the redshift uncertainty range $ZBEST_SIQR < 0.1$. The curves shown are results of fits based on Standard Cosmological Model [38] (red) and Segal's $\mathbb{R} \times S^3$ (green), using the same parameters as obtained in fits to the SCP "Union2.1" supernovae data shown in Figure 1, except for an additive constant.

225 The absorption coefficient α per single half-turn around the universe is closely related to the fraction of the
 226 celestial sphere obscured by galaxies distributed uniformly in a closed S^3 space. In Segal's simplest model, light is
 227 absorbed by matter present in N galaxies represented by black disks of radius r . Since the number of galaxies in the
 228 compact S^3 is finite, $\alpha \ll 1$. The total energy flux of light that has not been absorbed over n half-turns is $P e^{-\alpha n}$,
 229 where P is the energy flux of "pristine" light that did not yet travel by more than a half-turn around the universe.
 230 Summing a resulting power series over multiple half-turns around the universe gives

$$231 \quad P_{CMB} = \sum_{n=1}^{\infty} P e^{-\alpha n} = P/\alpha \quad (11)$$

232 since $\alpha \ll 1$. P is the energy flux of "pristine" light, emitted by N galaxies distributed uniformly in the universe,
 233 averaged over the entire universe and taking redshift into account. We calculated the average energy flux P following
 234 a geometrical analysis analogous to an estimate of the absorption coefficient α . The "pristine" light originates as light
 235 emitted by N galaxies, represented by disks of radius r and all of the same typical luminosity. In this simple model,
 236 the number of galaxies N , their radii r , and the radius of the 4-D hypersphere R , cancel out. As a result, one can
 237 express P_{CMB} in terms of the energy flux of light emitted by a typical galaxy at some distance from Earth, in terms
 238 of the radius of a typical galaxy radius r times a numerical factor. Since the spectrum of residual light is the Planck's

239 black-body distribution [23], one obtains a prediction for the temperature of the CMB from the Stefan-Boltzmann
240 law.

241 The observed value of the CMB temperature $T = 2.7 K$ can indeed be naturally explained. Taking the luminosity
242 of Milky Way, $L = 5 \times 10^{36} W/m^2$ for the luminosity of a typical galaxy, our simple model gives $T = 2.74 K$. (To
243 give a sense of sensitivity of this prediction to assumed typical luminosity, if one takes the luminosity of Andromeda
244 galaxy (*M31*) as that of a typical galaxy, the model gives $T = 3.2 K$, We note that Andromeda is a very bright
245 galaxy, most likely more luminous than an average galaxy in the universe.)

246 It is also appears possible to explain the main features of the observed power spectrum of CMB fluctuations as
247 due to the natural statistical distribution of the hierarchy of the large-scale structures in the universe - galaxy clusters,
248 superclusters, voids et cetera.

249 One can show that the main feature in the CMB power spectrum, the first peak at $l \sim 200$, can be reproduced
250 in this way, as shown In Figure 4. We have used a simple model in which galaxies are distributed according to a
251 hierarchical sequence of distances between superclusters, clusters and galaxies, with the distance scales taken from
252 existing observations, while keeping the number of galaxies per unit volume on large distance scales constant. We
253 generated a network of galaxies' positions in the sky, together with their corresponding energy fluxes, taking into
254 account reduction of the flux according to galaxies' distances from the observer, and their geometrical redshift. The
255 shape of the power spectrum is sensitive to the assumed distance scales between superclusters, clusters, galaxies, and
256 R , the "radius of the universe". We used software provided in the healpy package [45] to convert the sky coordinates
257 to obtain maps of the sky using a chosen HEALPix pixelization scheme, and then calculated the power spectra of
258 the simulated fluctuations. We used the pixelization scheme that was used for WMAP data, which did not have
259 very high angular resolution. We believe this choice was appropriate to explore whether the first peak of the power
260 spectrum can be explained by our very simple, preliminary model. Higher resolution data is available for future efforts
261 to reproduce higher order characteristics of power spectrum. More information about the theoretical predictions used,
262 and the fits themselves can be found in Appendix 2.

CONCLUSION

263 Segal's "Chronometric Cosmology", in which the geometry of the universe is spatially closed, finite and eternal,
264 provides an alternative explanation for cosmological redshift, and provides a verifiable prediction on the redshift-
265 distance dependence. We have compared the predictions of the Standard Model of Cosmology and Segal's universe

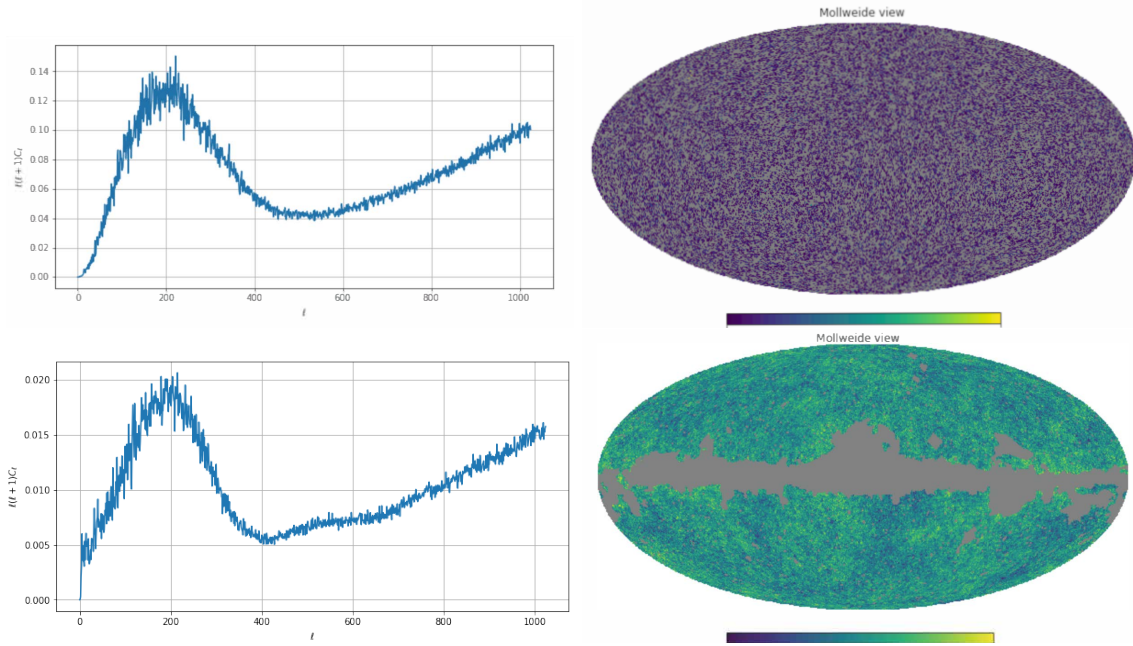


Figure 4: The simulated CMB power spectrum in Einstein-Segal universe (top left) calculated with healpy directly from a sky map of temperature fluctuations generated in Mathematica (top right) assuming a hierarchical distribution of galaxy superclusters, galaxy clusters and voids. For comparison, the corresponding CMB power spectrum calculated directly from WMAP is shown (bottom left) together with a WMAP data showing CMB temperature in our universe.

266 cosmology with data on cosmological redshifts, specifically $m(z)$ and $N(< z)$, and with the temperature and power
 267 spectrum of the CMB. Surprisingly, the data is consistent with predictions of Segal's $M = \mathbb{R} \times S^3$ universe.

268 We believe further research is merited into Segal's alternative explanation of the cosmological redshift and his
 269 Chronometric Cosmology model. Following a more detailed investigation of the consistency of observational data
 270 with alternative models of the universe, future work should explore the questions of conservation of energy, creation
 271 or recycling of matter and whether the distribution of elements observed in our universe could be explained in a
 272 spatially closed, static and eternal Segal-Einstein universe.

273 Additionally, the next few years will bring more data from the already operational James Webb Space Telescope
 274 (JWST), which will extend the reach and the resolution of studies of distant galaxies and objects at high redshifts.
 275 A dedicated study of the $N(< z)$ relation for chosen fixed angular cones in one of the Deep Fields could provide
 276 important information about the geometry of the universe. This observable is directly sensitive to the geometry
 277 of space, as shown in Figure 2. The JWST data could also provide important information about extinction and
 278 absorption of light emitted by distant sources, and the evolution of stars and galaxies in time, which at present
 279 introduce complications to the interpretation of both $m(z)$ and $N(< z)$ studies.

ACKNOWLEDGMENT

280 We thank Loring Tu for discussions, comments and a careful reading of the manuscript.

281 **Appendix 1: Fits to $m(z)$ relations**

282 In Figure 1, plotted are observed magnitudes as a function of redshift for the SCP "Union2.1" SN Ia compilation
283 data. The SCM prediction for $m(z)$, has been evaluated with the expression derived by Sandage [38], equation 33,
284 page 577:

$$285 \quad m_{\text{bol}}(z) = M_0 + 5\log_{10}\left(\frac{1}{q_o^2}(zq_o + (q_o - 1)(-1 + \sqrt{2q_o z + 1}))\right) + C \quad (12)$$

286 where $C = 2.5\log_{10}(4\pi) + 5\log_{10}\left(\frac{c}{H_o}\right)$, with speed of light c and Hubble constant H_o . The parameter q_o was set to the
287 value of $\frac{1}{2}$ for a flat universe and M_{bol} , the absolute brightness, was included with C as a free parameter. In addition,
288 we included in the fit a correction for the observed intensity to account for possible extinction, $I_{\text{corr}} = Ie^{-\lambda c\tau}$, which
289 gives an additional term $2.5\lambda\log_{10}(1+z)$ in the expression for $m_{\text{bol}}(z)$, where λ is the extinction coefficient, a free
290 parameter.

291 The prediction of Segal's for $m(z)$ has been obtained using the expression given by Segal [13] on page 94:

$$292 \quad m(z) = 2.5\log_{10}z - 2.5(2 - \alpha)\log_{10}(1+z) + C \quad (13)$$

293 where α is the power in the spectral function $f(\nu) \propto 1/\nu^\alpha$, where ν is the frequency. The parameter α was set to 1.
294 Setting α to some other value, say 2-3, gives almost identical results, except for a different value for the parameter λ ,
295 which is adjusted by the fit while leaving the fit quality almost identical. We also included in the fit a correction for
296 the observed intensity to account for possible extinction, which results in an additional term $5\lambda\log_{10}(e)\tan^{-1}(z^{1/2})$
297 in the expression for $m(z)$. The two fits have the same number of free parameters. Both fits are good, the values of
298 χ^2/dof , reported by Mathematica are 0.98 for SCM and 1.67 for Segal's model, where dof—the number of degrees
299 of freedom in the fit.

300 In Figure 3, plotted are the observed magnitude as a function of redshift for objects from one of Frontier Fields,
301 Abell A2744. The curves shown in this figure are based on results of fits obtained with Standard Cosmological
302 Model [38] (red) and Segal's $\mathbb{R} \times \mathbb{S}^3$ (green) and extrapolated to a wider redshift range. We have used the same
303 parameters as obtained in fits to the SCP "Union2.1" supernovae data shown in Figure 1, except for an additive
304 constant. Both curves describe the data well, however results are inconclusive. The values of χ^2/dof reported by
305 Mathematica are 2125.71 for SCM and 2092.68 for Segal's model.

306 **Appendix 2: CMB temperature and the first peak in the CMB power spectrum**

307 In Segal's model the CMB corresponds to "residual light", light that has not been absorbed over many turns
 308 around the universe. Following Segal's original approach, the absorption coefficient α is the fraction of the sky
 309 blocked by the randomly distributed N galaxies in S^3 , each with radius r . The 4-dimensional analogue of the polar
 310 angle in S^3 , at which all N galaxies should be placed to result in the same absorption coefficient as if they were
 311 uniformly distributed in S^3 space, is $\rho_{\text{eff}} = \pi/4$, or $\rho = 3\pi/4$. Since $\rho = l/R$, and $a = R\sin\rho$, it follows that the
 312 effective radius a_{eff} , the radius of a slice of S^3 at which one may place all N galaxies to give the same absorption, is

$$313 \quad a_{\text{eff}} = R\sin(\pi/4) = R\sin(3\pi/4) = R/\sqrt{2}. \quad (14)$$

314 The absorption coefficient α can be thus estimated by finding the ratio of areas obscured by N galaxies to the area
 315 of a slice of S^3 of the radius a_{eff} , or the area of a slice of S^3 at effective 4D polar angle ρ_{eff} :

$$316 \quad \alpha = N\pi r^2 / (\pi R^2 (1 - \cos^2 \rho_{\text{eff}} + \sin^2 \rho_{\text{eff}})) \quad (15)$$

$$317 \quad \alpha = N\pi \epsilon^2 / (\pi (1 - \cos^2(\pi/4) + \sin^2(\pi/4))) = N\pi \epsilon^2 / (\pi (1 - \cos^2(\pi/4) + \sin^2(\pi/4))) \quad (16)$$

318 which gives $\alpha = \epsilon^2 N/2$, where $\epsilon = r/R$.

319 As described in the main text, $\alpha \ll 1$ and the total energy flux of light that has not been absorbed over n
 320 half-turns is $P e^{-\alpha n}$, where P is the energy flux of "pristine" light. Summing a resulting power series gives

$$321 \quad P_{\text{CMB}} = \sum_{n=1}^{\infty} P e^{-\alpha n} = P/\alpha \quad (17)$$

322 To calculate the average flux of pristine light at a typical point of the S^3 universe, or the energy flux Φ emitted by
 323 N galaxies of luminosity L , randomly distributed in S^3 universe, we used the effective distance $a_{\text{eff}} = R\sin\rho_{\text{eff}}$ at
 324 which all N galaxies should be placed to give the same flux $\rho = \pi/4$ or $\rho = 3\pi/4$.

$$325 \quad \Phi = NL/(4\pi a^2) = NL/(2\pi R^2 (1 - \cos(\pi/4)^2 + \sin(\pi/4)^2)) = NL/(2\pi R^2) \quad (18)$$

326 P is the energy flux of "pristine" light, emitted by N galaxies distributed uniformly in the universe, averaged
 327 over the entire universe and taking redshift into account. The observed energy flux of the pristine light will be
 328 reduced by the redshift z . In Segal's model, after integration over the entire space, $\Phi_{\text{corr}} = P/2$. The luminosity of
 329 a typical galaxy L can be estimated from the energy flux of pristine light observed on Earth from Milky Way Φ_E ,
 330 $L = \phi_E 4\pi(r/2)^2$, where we took $r/2$ for the distance from Earth to Milky Way center. The expected flux of CMB
 331 is thus the product of corrected energy flux of pristine light at a typical point of the universe and the enhancement
 332

333 factor $1/\alpha$,

$$334 \quad P_{\text{CMB}} = \Phi_{\text{corr}}/\alpha = NL/(2\pi R^2)/(\epsilon^2 N/2)/2 = N(\Phi_E 4\pi(r/2)^2)/(2\pi R^2)/(\epsilon^2 N/2)/2 = \Phi_E/2 \quad (19)$$

335 Alternatively, one can take various estimates of luminosity of Milky Way, or Andromeda, and use their distance from
336 Earth to find the flux observed on Earth. For Andromeda, the expressions will be modified by the ratio of its distance
337 from Earth to the distance from Earth to the center of Milky Way. We obtained the temperature of a black body
338 corresponding to the predicted energy flux P_{CMB} using Stefan-Boltzmann law: $T = (P_{\text{CMB}}/\sigma)^{1/4}$, where σ is the
339 Stefan-Boltzmann constant.

340 The power spectrum for CMB characterizes two-point correlations between fluctuations of CMB temperature
341 measured in pixels according to a scheme defined in the healpy package. For the WMAP data, which detector had
342 limited angular resolutions, the number of pixels was smaller than for Planck data. We used the same pixelization
343 scheme to compare with WMAP, to allow a comparison of main features of the power spectrum with our crude
344 model. In our approach, we are adding up the energy flux from all sources, assumed to be galaxies of some typical
345 luminosity, falling into a given pixel. Since we are integrating over the entire volume of S^3 space, and account for the
346 dependence of the flux on the distance from the observer, this method provides an estimate of the average energy
347 flux of "pristine light in the universe. This flux is related to the energy flux of CMB. In Segal's model, CMB is the
348 residual light, not absorbed over many turns. It is larger than the average flux of pristine light by a factor $1/\alpha$, where
349 $\alpha \ll 1$ is the absorption coefficient, as described in the main text. However, the flux of pristine light a typical point
350 of the universe is smaller than the flux of pristine light on Earth, as Earth is located very close to the center of Milky
351 Way. This dilution factor is calculated similarly to the enhancement factor. As a result, since many factors cancel
352 out, the CMB flux in Segal's model is expected to be the product of some numerical factor f and the energy flux
353 from a typical galaxy at a chosen distance from an observer.

354 To generate the power spectrum we used a crude simulation with the number of superclusters $N_{\text{supercl}} \sim$
355 $(0.1 - 0.5) \times 10^6$, the number of clusters in a supercluster $N_{\text{cl}} = 7 - 10$, the number of galaxies in a cluster
356 $N_{\text{g}} \sim 20 - 50$, and the "radius of the universe" $R > 200 - 300$ Mps. The distance between superclusters was
357 assumed to be $D \sim 10$ Mps, and this value was taken as the "thickness" of S^3 slices, surfaces of spheres S^2 of
358 varying radii a . The distances between galaxy clusters and galaxies were obtained by scaling D by $1/N_{\text{cl}}$ and $1/N_{\text{g}}$,
359 correspondingly. The number of superclusters in each slice was taken such that the density of superclusters per unit
360 volume was kept approximately constant. In each slice of S^3 , we used Mathematica [46] to generate the supercluster
361 positions on the spheres of radii corresponding to a given slice of S^3 . The cluster positions were then distributed
362 randomly on a spherical surface surrounding the generated supercluster positions, using a typical distance between

363 clusters as the appropriately smaller radius. Finally, galaxies were randomly generated around the position of clusters
364 to which the galaxies belonged. Each generated galaxy has been assigned three coordinates (ρ, θ, ϕ) , which allows to
365 account for geometric effects and to calculate the energy flux reaching the observer, including those of the redshift.
366 To generate a projection on the "celestial sphere" we kept the two angular coordinates, (θ, ϕ) , after converting them
367 to the galactic coordinates.

368 Segal proved that the energy spectrum of light circulating multiple times around the universe will be a black-body
369 spectrum [23]. The total energy flux of the simulated pristine light falling into a given pixel, multiplied by the factor
370 f , gives the expected energy flux of CMB in a given pixel. Taking the fourth root of the simulated CMB energy
371 flux gives the temperature T of a black body that would give the same energy flux. In this way we obtained a
372 simulated pixelized map of CMB temperature. Finally, we used the healpy package to obtain the power spectrum of
373 the fluctuations of pixel temperatures.

374 The range of values that seem to reproduce the first peak in the CMB power spectrum at $l \sim 200$ is quite wide,
375 it is the ratios of the distance scales that are important. However, the sensitivity of the position of the first peak in
376 the CMB power spectrum to R opens a possibility, in principle, to estimate the range of values of R allowed by the
377 CMB data.

References

- [1] E. Hubble, "A Relation between Distance and Radial Velocity among Extra-Galactic Nebulae, Contributions from the Mount Wilson Observatory", Carnegie Institution of Washington, 310 1, (1927), and Proc.Nat.Acad.Sci. 15 (1929) 168-173
- [2] Edwin Hubble and Richard C. Tolman, "Two Methods of Investigating the Nature of the Nebular Red-shift", The Astrophysical Journal **82** (1935), pp. 302-337
- [3] I. Segal, "Covariant Chronogeometry and Extreme Distances. I", Astron. and Astrophys. **18** (1972) 143
- [4] Aubert Daigneault and Arturo Sangalli, "Einstein's Static universe: An Idea Whose Time Has Come Back?", Notices of the AMS, Vol. **48**, number 1, January 2000
- [5] A.H. Taub, book review of: "Mathematical cosmology and extragalactic astronomy," by Irving Ezra Segal, Pure and Applied Mathematics, vol. 68, Academic Press, New York, 1976, Bulletin of the American Mathematical Society, Volume **83**, Number 4, July 1977.
- [6] I. Segal, "A class of operator algebras which are determined by groups", Duke Math. J. 18, (1951) 221.
- [7] I. Segal, "Positive-energy particle models with mass splitting", Proc. Nat. Acad. Sci. U.S.A. 57, (1967) 194.
- [8] I. Segal, "Causally oriented manifolds and groups", Bull. Amer. Math. Soc. Vol. 77, number 6, (1971) 958
- [9] Irving Segal, "Causally connected manifolds and groups", Bull. Amer. Math. Soc. **77** (1971) 958
- [10] I. E. Segal, "A Variant of Special Relativity and Long-Distance Astronomy", Proc. Nat. Acad. Sci., **71** (1974) 765
- [11] I. E. Segal, "Observation validation of the chronometric cosmology: I. Preliminaries and the redshift-magnitude relation", Proc. Nat. Acad. Sci., **72** (1975) 2273
- [12] J. F. Nicoll and I. E. Segal, "Phenomenological analysis of the observed relations for low-redshift galaxies", Proc. Nat. Acad. Sci., **72** (1975) 2273
- [13] I. E. Segal, "Mathematical Cosmology and Extragalactic Astronomy", Academic Press, New York, 1976, Pure and Applied, Vol. 68
- [14] I. E. Segal, "Theoretical foundations of chronometric cosmology", Proc. Nat. Acad. Sci., **73** (1976) 669

- 403 [15] I. E. Segal, "Interacting quantum fields and the chronometric principle", Proc. Nat. Acad. Sci., **73** (1976) 3355
- 404 [16] Edward E. Fairchild, "The Segal Chronometric Redshift - A Classical Analysis", Astron. and Astrophys. **56**
405 (1977) 199
- 406 [17] I. E. Segal, "Correction to Erroneous Presentation of Chronometric Redshift Theory", Astron. and Astrophys.
407 **68** (1978) 343
- 408 [18] I. E. Segal, "Some recent tests of the chronometric cosmology", Proc. Nat. Acad. Sci., **77** (1980) 10
- 409 [19] I. E. Segal, "Time, energy, relativity and cosmology", in Symmetries in Science, B. Gruber et. al. (eds), Chapter
410 10, page 385, Plenum Press, New York, 1980
- 411 [20] Stephen M. Paneitz and Irving E. Segal, "Analysis in Space-Time Bundles. I. General Considerations and the
412 Scalar Bundle", J. Funct. Anal , **47** (1982) 457
- 413 [21] Stephen M. Paneitz and Irving E. Segal, "Analysis in Space-Time Bundles. II. The Spinor and Form Bundles",
414 J. Funct. Anal , **49** (1982) 335
- 415 [22] Stephen M. Paneitz and Irving E. Segal, "Analysis in Space-Time Bundles. III. Higher Spin Bundles", J. Funct.
416 Anal , **54** (1983) 18
- 417 [23] I. E. Segal "Radiation in the Einstein universe and the cosmic background", Phys. Rev. D. **28** (1983) 2393
- 418 [24] I. E. Segal, "Evolution of the Inertial Frame of the universe", Nuovo Cimento B **79** (1984) 187
- 419 [25] Laurence I. Wormald, "A Critique of Segal's Chronometric Theory", Gen. Relativ. Gravit. **16** (1984) 393
- 420 [26] I. E. Segal, "Concerning - A Critique of Segal's Chronometric Theory, by Laurence I. Wormald", Gen. Relativ.
421 Gravit. **16** (1984) 403
- 422 [27] I. E. Segal, "The redshift-distance relation", Proc. Nat. Acad. Sci., **90** (1993) 4798
- 423 [28] I. E. Segal, "Geometric derivation of the chronometric redshift", Proc. Nat. Acad. Sci., **90** (1993) 11114
- 424 [29] I. E. Segal and Z. Zhou, "Convergence of quantum electrodynamics in a curved modification of Minkowski
425 space", Proc. Nat. Acad. Sci., **91** (1994) 962
- 426 [30] I. E. Segal and Z. Zhou, "Maxwell's equations in the Einstein universe and chronometric cosmology", Astrophys.
427 J. Suppl., **S 100** (1995) 307

- 428 [31] Irving Segal and Zhengfang Zhou, "Conformal Extension of Massive Wave Functions", J. Funct. Anal , **155**
429 (1998) 550
- 430 [32] I. E. Segal, "Cosmological implications of a large complete quasar sample", Proc. Nat. Acad. Sci., **95** (1998)
431 4804
- 432 [33] I. E. Segal, "Is redshift-dependent evolution of galaxies a theoretical artifact?", Proc. Nat. Acad. Sci., **96** (1999)
433 13615
- 434 [34] I. E. Segal and J. F. Nicoll, "Astronomy phenomenological analysis of redshift-distance power laws", Astrophys.
435 Space Sci., **274** (2000) 503
- 436 [35] G. Darboux, "Memoire sur la theorie des coordonnees et des systemes orthogonaux", III; Annales Scientif. de
437 l'É.N.S. (Sér. 2) 7, 275-348 (1878)
- 438 [36] Aubert Daigneault, "Irving Segal's Axiomatization of Spacetime and its Cosmological Consequence", Invited
439 lecture given at the conference celebrating the 100th anniversary of the Hungarian mathematical logicians
440 László Kalmár and Rózsa Péter in Budapest, August 5, August 11, 2005
- 441 [37] Alexandrov, A.D. and Ovchinnikova, V.V., "Notes on the foundations of relativity theory", Vestnik Leningrad
442 Univ., 11 (1953), 95. ; Zeeman, E.C., "Causality implies the Lorentz group", Journal of Mathematical Physics,
443 5, (1964) 490-493
- 444 [38] A. Sandage, "Observational Tests of World Models". Annual Review of Astronomy and Astrophysics 26.1 (1988)
445 p. 561630
- 446 [39] Carroll, Sean M. ; Press, William H. ; Turner, Edwin L., "Cosmological Constant". Annual Rev. Astron. Astro-
447 phys., Vol. 30, p. 499-542 (1992)
- 448 [40] Suzuki et al (The Supernova Cosmology Project): "The Hubble Space Telescope Cluster Supernova Survey: V.
449 Improving the Dark Energy Constraints Above $z > 1$ and Building an Early-Type-Hosted Supernova Sample",
450 ApJ **746**, 85 (2012)
- 451 [41] M. Castellano et al., "The ASTRODEEP Frontier Fields Catalogues: II - Photometric redshifts and rest-frame
452 properties in Abell-2744 and MACS-J0416, Astron. & Astrophys. **590** (2016) A31
- 453 [42] Labbé, I. et al.: "A population of red candidate massive galaxies ~ 600 Myr after the Big Bang". Nature. **616**,
454 266 (2023)

- 455 [43] Carniani, S et al., "A shining cosmic dawn: spectroscopic confirmation of two luminous galaxies at $z \sim 14$ ".
456 arXiv:2405.18485 [astro-ph.GA]
- 457 [44] https://lambda.gsfc.nasa.gov/education/graphic_history/microwaves.html
- 458 [45] A. Zonca et al.: healpy: equal area pixelization and spherical harmonics transforms for data on the sphere in
459 Python, The Open Journal vol 4, 35 (2019) 1598; K. M. Gorski et al.: HEALPix: A Framework for High-
460 Resolution Discretization and Fast Analysis of Data Distributed on the Sphere, Astrophys.J vol **622** (2005)
461 759
- 462 [46] Wolfram Research, Inc., Mathematica, Version 14.0, Champaign, IL (2024).